Ab Initio Investigation of Structures and Energies of Low-Lying Electronic States of AlN_3, Al_3N, and Al_2N_2

Bong Hyun Boo* and Zhaoyang Liu

Department of Chemistry, Chungnam National University, Taejon 305-764, Korea, and Center for Molecular Science, 373-1 Kusung-dong, Yusung-gu, Taejon 305-701, Korea

Received: August 6, 1998; In Final Form: December 2, 1998

The structures and energies of low-lying electronic states of AlN_3, Al_3N, and Al_2N_2 have been evaluated at the HF, MP2, QCISD(T), CCSD, and CCSD(T) levels of theory, using the several basis sets of 6-31G* (for HF), cc-pVDZ (for MP2 and QCISD(T)), and cc-pVTZ (for CCSD and CCSD(T)). The ground state of AlN_3 is predicted to be a $^1\Sigma^+$ state with a linear Al−N−N−N structure. The most stable species of Al_3N is found, however, to have D_{3h} symmetry and $^1A_1'$ ground state. For Al_2N_2, various isomers are found to be energetically favorable. A rhombic isomer with the nitrogen atoms along the short diagonal and with a ^1A_g electronic state is the lowest in energy at the MP2/cc-pVDZ, QCISD(T)/cc-pVDZ, CCSD/cc-pVTZ, and CCSD(T)/cc-pVTZ levels. A linear structure Al−N−N−Al with a $^3\Sigma_g^-$ electronic state is the second lowest. The third stable isomer with the aluminum atoms bonded directly to the N_2 π orbital seems to be one of the model species for the sake of the nitrogen fixation. Our results suggest that the formation of a variety of the configuration of Al_2N_2 is energetically plausible under the reaction conditions employed since the energy differences in the Al_2N_2 species are relatively small.

Introduction

Clusters have been drawing a great deal of attention since clusters link the gap between isolated molecule and bulk material. Clusters containing III−V group elements such as GaAs,[1−4] BN,[5−22] AlP,[23,24] and InP[25] have been studied extensively due to their distinctive properties as precursors for bulk semiconductors. Among them, GaAs clusters have received much more attention due to the obvious technological importance.

Many workers have performed experiments to detect various BN cluster ions by applying intense laser to BN powders.[17−19] $B_{x+1}N_x^+$ ($x = 1 - 8$) series were detected when the supersonic expansion technique was employed to cool down the generated hot plasma.[19] Roland and Wynne also carried out photoionization and photofragmentation of $B_{x+1}N_x$ ($x = 1 - 8$) and found that the abundance of $B_{x+1}N_x^+$ increases as the laser intensity increases.[19]

However, less attention has been given to the generation of AlN cluster. Zheng and his co-workers have tried to generate AlN cluster ions in many ways and obtained only some small cluster ions when mixtures of aluminum and sodium azide were used as a sample for the laser ablation experiment.[26] This phenomenon is also observed under the similar experimental condition employing a boron and sodium azide mixture.[26] By a theoretical analysis by Seifert et al., based on linear combination of atomic orbital and local density approximation (LCAO-LDA),[20] these results may imply that the B_xN_y clusters were in the form of linear chains, which could dissociate exothermically into N_2 and the corresponding cluster ions when two or more N atoms were adjacent to one another in the BN chain.

In this report, we have emphasized theoretically the elucidation of the structure, bond strength, and energies of low-lying electronic states of AlN_3, Al_3N, and Al_2N_2. We have checked all possible geometries of the aluminum nitrides to find local minima on the potential energy surfaces at the HF and MP2 levels, and then predicted the energies with the higher levels of QCISD(T), CCSD, and CCSD(T). It is reported that the QCISD(T) energy is close to the full configuration interaction one.[27] Specially, results on molecules with stretched bond are improved.[27] It is also known that that such a CCSD(T)/cc-pVTZ calculation is more accurate in evaluation of the energy difference.[28]

This theoretical study will shed some new light on the preparation condition of the cluster isomers having different structures, which would consequently have different properties of macroscopic AlN materials.

Computational Methods

The geometric parameters for all the different starting structural and electronic (singlet and triplet) arrangements were optimized completely using a gradient technique at the Hartree−Fock (HF) level of theory.[29] Initial optimization was performed using the 6-31G* basis set at the HF level.[30] For the promising structures, the final optimization was performed using the correlation consistent polarized valence double ζ (cc-pVDZ) basis set of Dunning[31,32] at the second-order Møller−Plesset (MP2) perturbation theory.[33−35] All electrons are included in the correlation energy calculations for all the configurations of AlN_3, Al_2N_2, and Al_3N.

For each structure, the complete sets of harmonic vibrational frequencies were then evaluated using the analytical second derivative techniques at both the HF/6-31G* and MP2/cc-pVDZ levels. The harmonic vibrational frequencies were used to determine whether a given structure is a local minimum on the potential energy surface or not and to perform a zero point energy (ZPE) correction.

* Author to whom correspondence should be addressed.

10.1021/jp983297k CCC: $18.00
Published on Web 02/17/1999

In order to obtain more reliable relative energies, additional calculations were carried out for all the species with the quadratic configuration interaction technique including the corrections for triple excitations [QCISD(T)].[27,36] This technique is known to be accurate even for complicated systems where the electron correlation effects are extremely important.[36]

At the final geometries, additional single point energy calculations were also performed at the CCSD [the coupled-cluster (CC) with all single and double substitutions],[37−39] and CCSD(T) (the coupled-cluster with all single and double substitutions, and a quasi-perturbative estimate for the effect of connected triple excitations) levels.[36,37,39−41] The basis set used for the CC calculation is the correlation consistent polarized valence triple ζ (cc-pVTZ) basis set of Dunning.[31,32] It is well-known that the CCSD(T) method is a reliable and cost-efficient technique for ab initio quantum chemistry[40−42] and that the CCSD(T) level of theory estimates energies very close to full configuration interaction[37] when the nondynamical correlation effects are not very important.[38,40]

To estimate the bond strengths in the tetraatomic species, we have optimized structures of singlet or triplet Al_2, AlN, and N_2 at the MP2 level and then obtained their total energies (including ZPE obtained at the MP2 level) at the levels of QCISD(T)/cc-pVDZ//MP2/cc-pVDZ, CCSD/cc-pVTZ//MP2/cc-pVDZ, and CCSD(T)/cc-pVTZ//MP2/cc-pVDZ. It is noticed that inner shells are excluded from the correlation energy calculation at the CCSD and CCSD(T) levels on all the di- and tetraatomic species due to the computation time. All the calculations were carried out using the Gaussion 94 program suite[43] on a Cray c90 supercomputer installed at SERI.

Results and Discussion

All possible combinations of AlN_3, Al_3N, and Al_2N_2 are searched at the HF and MP2 levels. However, in some cases, the geometrical optimization of many different starting configurations is found to give the same geometrical parameters upon optimization. In Figure 1, we presented their final geometrical structures, including only real harmonic vibrational frequencies. Here, A, B, and C notations indicate the three geometrical species of AlN_3, Al_3N, and Al_2N_2, respectively, and $i = 1, 2, 3, \ldots$ refers to the corresponding structural isomers as indicated Figure 1, the numbers following the energetic order.

In Table 1, we list the total energies (including ZPE) calculated at the HF/6-31G*, MP2/cc-pVDZ, QCISD(T)/cc-pVDZ//MP2/cc-pVDZ, CCSD/cc-pVTZ//MP2/cc-pVDZ, and CCSD(T)/cc-pVTZ//MP2/cc-pVDZ levels. Table 2 lists the harmonic vibrational frequencies along with their intensities and approximate mode descriptions. Almost all the modes in the cyclic species are delocalized over whole molecule and thus cannot be assigned to several local vibrations. This is a characteristic feature of cyclic compounds.[44] It is shown in the intensity and mode analyses that the fundamentals involving the N−Al stretch are relatively intense, correctly reflecting the large electronegativity difference between N and Al.

The relative energy orderings are the same at all the levels examined except the HF level. This indicates that the electron correlation calculation is very important in the evaluation of the electronic energy. It is noticed that all the energy values used in this text refer to the scaled CCSD(T)/cc-pVTZ energies, unless noted otherwise. To check whether the optimized structures are below the dissociation limit or not, we have also estimated the bond strengths in the low-lying states from the total energies of Al_2, AlN, and N_2 evaluated in this study. In Table 3, we list the total energies (including ZPE) of the ground states. The bond strengths in the tetraatomic species are discussed in comparison with those in the diatomic species obtained from the thermochemical table (Table 4).

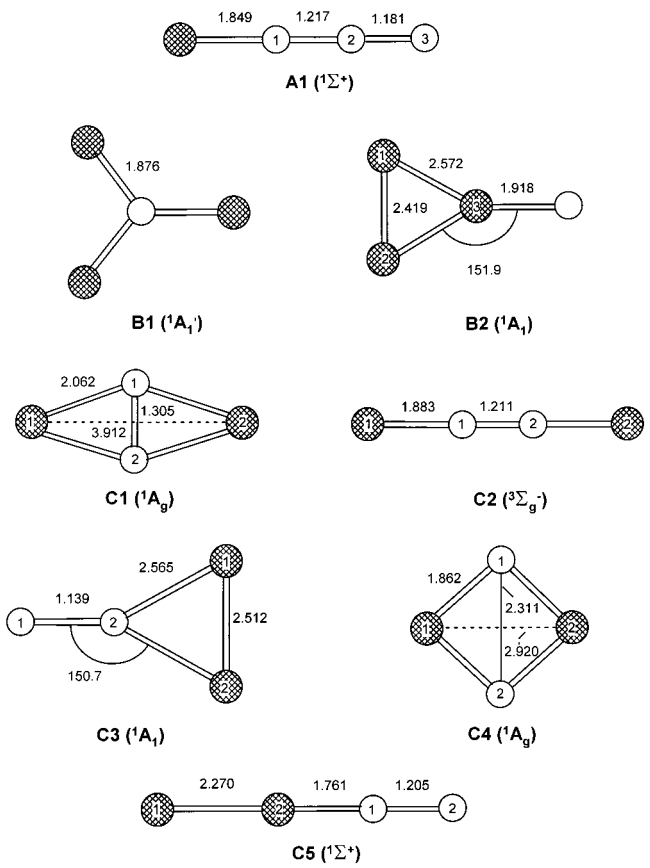

Figure 1. Structures of low-lying electronic states of AlN_3 (Ai), Al_3N (Bi), and Al_2N_2 (Ci) after the optimization at the MP2 level, i indicates the structure number. Open circles represent N atoms, and shaded circles represent Al atoms.

AlN_3. As shown in Figure 1, we obtained only one optimized geometry including real harmonic frequencies, as listed in Table 2. As shown in Table 1, the linear AlN_3 ($^1\Sigma^+$) with the aluminum atom positioned at one terminal is the most stable species at all the levels examined. For this structure, there is an imaginary vibrational frequency at the HF/6-31G* level. However, at the higher level MP2/cc-pVDZ where the correlation energy correction is considered, no imaginary frequency is found. The previous studies of BN_3, a structural analog of AlN_3, show that the most stable configuration is a linear NNBN having a clear-cut $^1\Sigma^+$ ground state.[5] We have also optimized this geometry for AlN_3 and then obtained a very long NN−AlN bond length (4.485 Å at the HF/6-31G* level). This suggests that the species tends to dissociate into AlN and N_2. This is reflected from the different bond strengths of the Al−N and B−N bonds. In the case of NAl−NN, the strong N−N interaction can compensate the cleavage of the weaker NN−AlN bond.

For the A1 structure, we estimated the bond strength (D_0^0(AlN−NN)] from the total energies listed in Tables 1 and 3 as 50 kcal/mol, being much lower than the normal N≡N bond energy (225.06 ± 0.03 kcal/mol), the value derived from a literature thermochemical table[45] (Table 4). This weak bond strength correctly reflects the corresponding longer bond length (1.217 Å), as shown in Figure 1. The N−N−N stretching fundamental (Al is almost not in motion) is predicted as 2220 cm^{-1} as the highest fundamental in all the species, and close to the N−N stretching frequency 2358 cm^{-1} of the gas phase N_2.

TABLE 1: Total Energies (Hartree), Including the Zero Point Energy, and Relative Energies (kcal/mol) for Low-Lying Electronic States of AlN_3, Al_3N, and Al_2N_2

species	structure	point group	electronic state	total energies (hartree) HF/6-31G*	MP2/cc-pVDZ	QCISD(T)/cc-pVDZ	CCSD/cc-pVTZ	CCSD(T)/cc-pVTZ	relative energies (kcal/mol) HF	MP2	QCISD(T)	CCSD	CCSD(T)
AlN_3	Al	$C_{\infty v}$	$^1\Sigma^+$	−405.186 784	−405.778 907	−405.799 936	−405.914 679	−405.956 321	0	0	0	0	0
Al_3N	B1	D_{3h}	$^1A_1'$	−780.211 939	−780.582 573	−780.630 678	−780.696 727	−780.718 847	0	0	0	0	0
	B2	C_{2v}	$^1A_1$	−779.918 773	−780.283 635	−780.350 082			184	188	176		
Al_2N_2	C1	D_{2h}	^1A_g	−592.665 175	−593.134 196	−593.179 180	−593.268 962	−593.299 422	0	0	0	0	0
	C2	$D_{\infty h}$	$^3\Sigma_g^-$	−592.667 908	−593.110 176	−593.159 937	−593.253 784	−593.280 978	-1.7	15	12	9.5	12
	C3	C_{2v}	$^1A_1$	−592.629 479	−593.105 406	−593.151 499	−593.226 424	−593.260 853	22	18	17	27	24
	C4	D_{2h}	^1A_g	−592.497 782	−593.063 189	−593.089 607	−593.170 665	−593.225 631	105	45	56	62	46
	C5	$C_{\infty v}$	$^1\Sigma^+$	−592.445 989	−592.970 064	−593.049 160	−593.075 317	−593.169 512	138	103	82	122	82

TABLE 2: Harmonic Vibrational Frequencies Calculated at the MP2/cc-pVDZ Level[a]

cluster	structure	vibrational frequencies (cm^{-1}) (sym, intensity (km/mol), approx mode description)
AlN_3	A1	39 (π, 1, bending), 489 (σ, 166, Al−N str), 560 (π, 13, bending), 1376 (σ, 139, str), 2220 (σ, 687, str)
Al_3N	B1	149 (e′, 4, ip bending), 187 (a_2'', 0, oop bending), 417 (a_1', 0, tot sym str), 740 (e′, 329, str)
	B2	109 (b_2, 9, ip bending), 154 (b_1, 11, oop bending), 297 (a_1, 0, tot sym ip bending), 301 (b_2, 2, ip bending), 406 (a_1, 0, tot sym str), 707 (a_1, 47, tot sym N−Al str)
Al_2N_2	C1	164 (b_{3u}, 0, oop bending), 227 (b_{2u}, 20, ip bending), 353 (a_g, 0, tot sym str along the Al−Al axis), 594 (b_{3g}, 0, ip bending), 605 (b_{1u}, 513, ip bending), 1276 (a_g, 0, tot sym str along the N−N axis)
	C2	119 (π_u, 1, bending), 354 (π_g, 0, bending), 366 (σ_g, 0, tot sym str), 661 (σ_u, 535, N−Al str), 1721 (σ_g, 0, tot sym str)
	C3	66 (a_1, 4, Al_2-N_2 str), 80 (b_2, 3, ip bending), 172 (b_2, 1, ip AlNN bending), 242 (b_1, 98, oop bending), 340 (a_1, 0, tot sym Al−Al str), 2024 (a_1, 249, tot sym N−N str)
	C4	89 (b_{3u}, 70, oop bending), 390 (a_g, 10, tot sym ring def), 643 (b_{3g}, 0, ring def), 705 (a_g, 0, ring puckering), 755 (b_{2u}, 1296, ip bending), 930 (b_{1u}, 60, ip bending)
	C5	58 (π, 2, bending), 341 (π, 4, bending), 389 (σ, 4, Al−Al str), 687 (σ, 266, tot sym N−Al and Al−Al str), 1269 (σ, 3283, tot sym N−N and N−Al str)

[a] ip refers to in-plane, and oop, to out-of-plane.

TABLE 3: Total Energies (Hartree) Including the Zero Point Energy for the Ground States of Al_2, AlN, and N_2

cluster	electronic state	total energies (hartree) MP2/cc-pVDZ	QCISD(T)/cc-pVDZ	CCSD/cc-pVTZ	CCSD(T)/cc-pVTZ
Al_2	$^3\Sigma^-$	−483.753 389	−483.789 525	−483.798 545	−483.809 591
AlN	$^1\Sigma^+$	−296.380 819	−296.454 564	−296.480 695	−296.507 971
N_2	$^1\Sigma_g^+$	−109.262 209	−109.274 580	−109.350 400	−109.368 882

TABLE 4: Enthalpies of Formation in kcal/mol at 0 K

species	$\Delta_f H_0^0$
AlN(g)	125(9.1)
Al_2(g)	116.2(0.8)
N_2(g)	0(0)
Al(g)	78.2(1.0)
N(g)	112.53(0.02)

[a] Ref 45.

This indicates that the terminal N—N bond may involve a triple bond character.

Al_3N. For Al_3N, two isomers of Al_3N without imaginary frequencies are found upon the geometrical optimization at the MP2 level. In contrast to AlN_3, the most stable isomer B1 involves a D_{3h} geometry and $^1A_1'$ ground state having the Al−N bond length of 1.876 Å.

The other isomer without any imaginary harmonic vibrational frequency is a $^1A_1$ ground state having a C_{2v} symmetry, which is labeled B2 in Figure 1, and is 176 kcal/mol much higher in energy than the D_{3h} ground state at the QCISD(T) level. Unfortunately, we could not obtain the CC energies at this MP2-optimized geometry. The Al^1-Al^3 bond strength is estimated as 33 kcal/mol at the QCISD(T) level, the value compared with a spectroscopic value of $D_0^0 = 30.9 \pm 1.4$ kcal/mol.[46] Therefore we presume that the B2 configuration is below the dissociation limit to Al_2 and AlN.

The QCISD(T) calculation indicates that a singlet quasilinear Al−Al−N−Al structure is 60 kcal/mol higher in energy than the most stable one. In the case of B_3N, however, the linear configuration is the most stable one.[22] Interestingly, the isomer with the same structure but the different electronic state $^3\Sigma^-$ of Al−N−Al−Al is much higher by 56 kcal/mol in energy than the corresponding singlet state at the QCISD(T)/cc-pVDZ level. Comparing the geometrical parameters of the two singlet and triplet isomers, it is found that in the $^3\Sigma^-$ electronic state, the two terminal Al−Al and N−Al bonds and the central Al−N bond lengths are shortened significantly. The changes in the bond length imply that the triplet species has a cumulene-like linear Al−Al−N−Al structure. Although these two linear structures are energetically favored, the existence of two imaginary harmonic vibrational frequencies at the MP2 level implies that they are not real minima on the potential surfaces.

Al_2N_2. In a previous study of B_2N_2, several structure with linear BNBN ($^3\Pi$) and rhombic $^3B_{2g}$ states have been found to be energetically competitive, while both the B−N−B−N ($^3\Pi$) and B−B−N−N ($^3\Pi$) species have been observed experimentally.[21] In the case of Al_2P_2, the lowest energy structure is a rhombus with the phosphorus atoms positioned along the short diagonal with a ^1A_g ground state.[23]

As expected, the most stable isomer of Al_2N_2 is found to be the rhombic one, which includes the nitrogen atoms along the short diagonal with a ^1A_g electronic state, and is more stable than the linear one with $^3\Sigma_g^-$ state by 15, 12, 9.5, and 12 kcal/mol at the MP2, QCISD(T), CCSD, and CCSD(T) levels, respectively. This suggests that the consideration of electron

correlation is important in the evaluation of the stability of Al_2N_2 isomers. In the C1 structure, the totally symmetric N−N stretch along the shorter axis (the N−N axis) is predicted at 1276 cm^{-1}. This indicates that a strong interaction occurs between the N atoms, reflecting the shorter bond length.

Checking the bond lengths in the linear configuration (C2), we predicted that both the Al−N and N−N bonds have a double bond character. The bonding parameters are reflected from the corresponding bond strength D_0^0(AlN−NAl) = 172 kcal/mol. Thus we presume that the AlN−NAl bond is close to a double bond. The fundamental at 1721 cm^{-1} is due to a symmetric N−N stretch, indicating that relatively strong chemical forces are exerted on the N atoms. The same linear structure, but with the different electronic state $^1\Sigma_g^+$ is 22 kcal/mol higher than the lowest one at the QCISD(T) level. Unfortunately, the MP2 level optimization does not provide a unique optimized structure having the lowest linear singlet state.

The C3 structure with a $^1A_1$ electronic state under C_{2v} point group follows in the stability the rhombic and linear structures. In the previous investigation on the tetratomic III−V group clusters such as B_2N_2,[21] Al_2P_2,[23] and Ga_2As_2,[3] none of the literature has considered this structure. The N−N bond length is rather short, only 1.139 Å at the MP2/cc-pVDZ level, which is the shortest among all these isomers of Al_2N_2 and close to the triple bond length (1.0977 Å). On the other hand, the Al−N bond length is the longest one. These bonding characters indicate that, in this structure, the Al−N bond is weak. The formation of this interesting structure can be explained by the d orbital participation of the Al atoms in the bonding directly with the π orbital of N_2. This may provide a new insight into the nitrogen fixation because of the stable behavior of this configuration. As expected, the Al_2−NN bond strength in the C3 structure is 57 kcal/mol. The fundamental at 2024 cm^{-1} corresponds to a totally symmetric N−N stretch and close to the N_2 stretching frequency, indicating that the N−N bond in the C3 structure may involve a triple bond character, reflecting the shorter bond length. The fundamental at 340 cm^{-1} corresponds to the Al−Al stretch, and a little lower than the Al−Al stretching frequency 479 cm^{-1} in the gas phase Al_2 obtained at the MP2 level. This indicates that the Al−Al bond in the C3 structure is a little weaker than the Al−Al bond in Al_2(g).

According to the suggestion of Al-Laham et al.,[23] we treat the rhombic structure with the ^1A_g electronic state by gradually increasing the N−N bond length and simultaneously decreasing the Al−Al one and then obtained one more conformer with the configuration C4. The total energy of Al_2N_2 with D_{2h} symmetry increases with increasing N−N bond length. This suggests that the interaction of N−N is very important in the stabilization of the D_{2h} Al_2N_2. The second rhombic structure (C4) with aluminum atoms located at the shorter diagonal and electronic state (^1A_g) are 46 kcal/mol higher in energy than the most stable one. The vibrational mode analysis indicates that the totally symmetric ring puckering occurs at 705 cm^{-1}, being much lower than the N−N stretching fundamental in N_2(g). This implies that a weak interaction exists between the N atoms.

Besides these, another linear isomer, Al—Al—N—N (C5) with a $^1\Sigma^+$ electronic state is obtained, which is 82 kcal/mol higher in energy than the most stable rhombic one. The bond strength corresponding to the Al—N bond is estimated to be 0 kcal/mol, indicating that this structure reaches the dissociation limit to Al_2 and N_2. It is noticed that the Al—N bond strength in the gas phase AlN is 66 ± 9 kcal/mol, the value derived from the JANAF table[45] (Table 4). It is predicted that the fundamental at 1269 cm^{-1} involves N—N and N—Al stretches, indicating that the chemical force in the N—N bond is not so strong as that in the N≡N bond in N_2(g).

We have also examined another linear Al−N−Al−N with the singlet and triplet multiplicities. The MP2 calculation shows that the singlet one is slightly bent, and an imaginary harmonic vibrational frequency is found. In the case of triplet one, no convergence in the structure optimization can be achieved.

Combining these results with the fact that the bond nature of Al−N lies between those of B−N and Al−P bonds, we expect that both the linear and rhombic configurations of Al_2N_2 should coexist, and the transformation of Al_2N_2 between the linear and rhombic structures is possible under a certain reaction condition. These energetic behaviors of the cluster seem to be very important in determining the reaction condition for the preparation of bulk materials consisting of the aluminum and nitrogen atoms with a ratio of 1:1, since the different structures of Al_2N_2 could lead to different properties of the material.

Conclusions

In this report, we present initial theoretical results on tetraatomic aluminum nitride clusters. All the possible geometries were taken into consideration with the singlet and triplet multiplicities at the HF/6-31G* level. The promising configurations were reoptimized at the MP2/cc-pVDZ level with a full electron correlation included. The harmonic vibrational frequencies were also calculated. Finally, the electronic energies were evaluated at the QCISD(T)/cc-pVDZ, CCSD/cc-pVTZ, and CCSD(T)/cc-pVTZ on the MP2-optimized parameters. The total energies scaled by the ZPE energies obtained at the HF or MP2 methods are listed in Table 1.

Vibrational frequency and mode analyses are quite informative as to the chemical forces among the atoms. The relative energy orderings are the same at all the levels employed, except the HF level.

Only a few stable isomers are achieved for the AlN_3 and Al_3N systems. The most stable AlN_3 involves an aluminum azide type having the linear AlNNN structure with the $^1\Sigma^+$ ground state. For Al_3N, the $^1A_1'$ isomer with D_{3h} symmetry is the lowest in energy. In the case of Al_2N_2, more isomers are found, and some of them are very close to each other in energy. The higher level single point calculations on the MP2-optimized structures indicate that a rhombic structure including the nitrogen atoms along the short diagonal and ^1A_g ground state is the lowest in energy, and the linear Al−N−N−Al with the $^3\Sigma_g^-$ electronic state is the second lowest. However, the energy difference between the rhombic and linear structures is small. The third one, which was not found in the previous calculation on the other tetratomic III−V group clusters, is found to have C_{2v} point group and an $^1A_1$ electronic state, which can be viewed as the Al-bonded directly to the π orbital of N_2.

Acknowledgment. The present studies were supported by the Korea Atomic Energy Research Institute and were partially supported by the Ministry of Education, Korea, through the Basic Science Research Institute Program, 1997-1998, Project No. BSRI-97-3432. B.H.B. is grateful to the Center for Molecular Science (CMS) for partial financial support. Computations in the present work are carried out by using the CRAY C90 of the SERI Supercomputer Center in Korea, which is gratefully acknowledged.

References and Notes

(1) O'Brien, S. C.; Liu, Y.; Zhang, Q.; Heath, J. R.; Tittel, F. K.; Curl, R. F.; Smalley, R. E. *J. Chem. Phys.* **1986**, *84*, 4074.

(2) Lemire, G. W.; Bishea, G. A.; Heidecke, S. A.; Morse, M. D. *J. Chem. Phys.* **1990**, *92*, 121.
(3) Meier, U.; Peyerimhoff, S. D.; Grien, F. *Chem. Phys*. **1991**, *150*, 331.
(4) Lou, L.; Wang, L.; Chibante, L. P. F.; Laaksonen, R. T.; Nordlander, P.; Smalley, R. E. *J. Chem. Phys*. **1991**, *94*, 8015.
(5) Martin, J. M. L.; Slanina, Z.; Francois, J.-P.; Gijbels, R. *Mol. Phys*. **1994**, *82*, 155.
(6) Martin, J. M. L.; El-Yazal, J.; Francois, J.-P.; Gijbels, R. *Chem. Phys. Lett*. **1995**, *232*, 289.
(7) Martin, J. M. L.; El-Yazal, J.; Francois, J.-P.; Gijbels, R. *Mol. Phys*. **1995**, *85*, 527.
(8) Martin, J. M. L.; El-Yazal, J.; Francois, J.-P. *Chem. Phys. Lett*. **1996**, *248*, 95.
(9) Jensen, F.; Toftlund, H. *Chem. Phys. Lett*. **1993**, *201*, 89.
(10) Jensen, F. *Chem. Phys. Lett*. **1993**, *209*, 417.
(11) Wang, B.-C.; Yu, L.-J.; Wang, W.-J. *Int. J. Quantum Chem*. **1996**, *57*, 465.
(12) Sutjianto, A.; Pandey, R.; Recio, J. M. *Int. J. Quantum Chem*. **1994**, *52*, 199.
(13) Fowler, P. W.; Heine, T.; Mitchell, D.; Schmidt, R.; Seifert, G. *J. Chem. Soc., Faraday Trans*. **1996**, *92*, 2197.
(14) Silaghi-Dumitrescu, I.; Lara-Ochoa, F.; Bishof, P.; Haiduc, I. *J. Mol. Struct*. (*Theochem*) **1996**, *367*, 47.
(15) Silaghi-Dumitrescu, I.; Lara-Ochoa, F.; Haiduc, I. *J. Mol. Struct*. (*Theochem*) **1996**, *370*, 17.
(16) Shao, Y.; Jiang, Y. *J. Phys. Chem*. **1996**, *100*, 1554.
(17) Becker, S.; Dietz, H.-J. *Int. J. Mass Spectrom. Ion Processes* **1986**, *73*, 157.
(18) Becker, S.; Dietz, H.-J.; Kessler, G.; Bauer, H.-D.; Pompe, W. *Z. Phys. B* **1990**, *81*, 47.
(19) Roland, P. A.; Wynne, J. J. *J. Chem. Phys*. **1993**, *99*, 8599.
(20) Seifert, G.; Schwab, B.; Becker, S.; Dietze, H.-J. *Int. J. Mass Spectrom. Ion Processes* **1988**, *85*, 327.
(21) Andrews, L.; Hassanzadeh, P.; Burkholder, T. R.; Martin, J. M. L. *J. Chem. Phys*. **1993**, *98*, 922.
(22) Slanina, Z.; Martin, J. M. L.; Francois, J.-P.; Gijbels, R. *Chem. Phys. Lett*. **1993**, *201*, 54.
(23) Al-Laham, M. A.; Trucks, G. W.; Raghavachari, K. *J. Chem. Phys*. **1992**, *96*, 1137.
(24) Tomasulo, A.; Ramakrishna, M. V. *J. Chem. Phys*. **1996**, *105*, 10449.
(25) Kolenbrander, K. D.; Mandich, M. L. *J. Chem. Phys*. **1990**, *92*, 4759.
(26) Zheng, L. S. Unpublished results.
(27) Pople, J. A.; Head-Gorden, M.; Raghavachari, K. *J. Chem. Phys*. **1987**, *87*, 5968.
(28) Lee, T. J.; Scuseria, G. E. Achieving Chemical Accuracy with Coupled-Cluster Theory in *Quantum Mechanical Electronic Structure Calculations with Chemical Accuracy*; Langhoff, S. R., Ed.; Kluwer: Dordrecht, The Netherlands, 1995.
(29) For a general introduction to Hartree−Fock-based methods, see: Hehre, W. J.; Radom, L.; Schleyer, P. v. R.; Pople, J. A. *Ab initio Molecular Orbital Theory*; Wiley: New York, 1986.
(30) Francl, M. M.; Pietro, W. J.; Hehre, W. J.; Binkley, J. S.; Gordon, M. S.; DeFrees, D. J.; Pople, J. A. *J. Chem. Phys*. **1982**, *77*, 3654.
(31) Dunning, T. H., Jr. *J. Chem. Phys*. **1989**, *90*, 1007.
(32) Woon, D. E.; Dunning, T. H., Jr. *J. Chem. Phys*. **1993**, *98*, 1358.
(33) Head-Gordon, M.; Pople, J. A.; Frisch, M. J. *Chem. Phys. Lett*. **1988**, *153*, 503.
(34) Frisch, M. J.; Head-Gordon, M.; Pople, J. A. *Chem. Phys. Lett*. **1990**, *166*, 275.
(35) Frisch, M. J.; Head-Gordon, M.; Pople, J. A. *Chem. Phys. Lett*. **1990**, *166*, 281.
(36) Raghavachari, K.; Trucks, G. W.; Pople, J. A.; Replogle, E. *Chem. Phys. Lett*. **1989**, *158*, 207.
(37) Watts, J. D.; Gauss, J.; Bartlett, R. J. *J. Chem. Phys*. **1993**, *98*, 8718.
(38) Lee, T. J.; Rendell, A. P.; Taylor, P. R. *J. Phys. Chem*. **1990**, *94*, 5463.
(39) Seidl, E. T.; Schaefer, H. F. *J. Chem. Phys*. **1992**, *96*, 4449.
(40) Scuseria, G. E.; Lee, T. J. *J. Chem. Phys*. **1990**, *93*, 5851.
(41) Scuseria, G. E. *Chem. Phys. Lett*. **1991**, *176*, 27.
(42) Ragavachari, K.; Trucks, G. W.; Pople, J. A.; Head-Gordon, M. *Chem. Phys. Lett*. **1989**, *157*, 479.
(43) Frisch, M. J.; Trucks, G. W.; Schlegel, H. B.; Gill, P. M. W.; Johnson, B. G.; Robb, M. A.; Cheeseman, J. R.; Keith, T.; Petersson, G. A.; Montgomery, J. A.; Raghavachari, K.; Al-Laham, M. A.; Zakrzewski, V. G.; Ortiz, J. V.; Foresman, J. B.; Cioslowski, J.; Stefanov, B. B.; Nanayakkara, A.; Challacombe, M.; Peng, C. Y.; Ayala, P. Y.; Chen, W.; Wong, M. W.; Andres, J. L.; Replogle, E. S.; Gomperts, R.; Martin, R. L.; Fox, D. J.; Binkley, J. S.; Defrees, D. J.; Baker, J.; Stewart, J. P.; Head-Gordon, M.; Gonzalez, C.; Pople, J. A. *Gaussian 94*, Revision D.2; Gaussian, Inc.: Pittsburgh, PA, 1995.
(44) Szczepanski, J.; Vala, M.; Talbi, D.; Parisel, O.; Ellinger, Y. *J. Chem. Phys*. **1993**, *98*, 4494.
(45) Chase, M. W., Jr., et al. *J. Phys. Chem. Ref. Data*, **1985**, *14*, suppl. 1(JANAF Thermochemical Tables).
(46) Fu, Z.; Lemire, G. W.; Bishea, G. A.; Morse, M. D. *J. Chem. Phys*. **1990**, *93*, 8420.